Gas sensitivity properties of TiO_2/Ag nanocomposite films prepared by pulse laser deposition

Nassar A. Al-Isawi[1], Kadhim A. Aadim[2], Ali A. Yousif[3]

[1]Ecology Department, Collage of Science, University of Al-Qadisiya

[2]Department of Physics, Collage of Science, University of Baghdad

[3]Department of Physics, College of Education, University of Al-Mustansiriyah

E-mail: nassar.al.isawi@qu.edu.iq

Abstract

In this study, a double frequency Q-switching Nd:YAG laser beam (1064 nm and λ= 532 nm, repetition rate 6 Hz and the pulse duration 10ns) have been used, to deposit TiO_2 pure and nanocomposites thin films with noble metal (Ag) at various concentration ratios of (0, 10, 20, 30, 40 and 50 wt.%) on glass and p-Si wafer (111) substrates using Pulse Laser Deposition (PLD) technique. Many growth parameters have been considered to specify the optimum condition, namely substrate temperature (300˚C), oxygen pressure (2.8×10^{-4} mbar), laser energy (700) mJ and the number of laser shots was 400 pulses with thickness of about 170 nm. The surface morphology of the thin films has been studied by using atomic force microscopes (AFM). The Root Mean Square (RMS) value of thin films surface roughness increased with increasing of Ag contents, while the crystallite size was found to decrease with increase in different silver content. The sensitivity toward NO_2 and NH_3 gas has been measured under different ppm concentrations. TiO_2 with noble metal has a sensitivity higher than pure TiO_2 where as TiO_2 with Ag metal deposited on glass substrate has maximum sensitivity to NO_2 gas with a value of ~(50 %) at the nanocomposite $_{90\%}TiO_2/_{10\%}Ag$ films with best operation temperature at 200 °C. In addition, noble metal like Ag to the titanium dioxide materials makes them sensitive to NO_2 gas.

Key words

Titanium oxide, morphology and sensitivity properties, PLD technique.

Article info.

Received: Mar. 2017
Accepted: Mar. 2017
Published: Dec. 2017

خصائص المتحسس الغازي للغشاء المتراكب النانوي TiO_2/Ag المحضر بطريقة الليزر النبضي

نصار عبد الامير العيساوي[1]، كاظم عبد الواحد عادم[2]، علي احمد يوسف[3]

[1]قسم البيئة، كلية العلوم، جامعة القادسية

[2]قسم الفيزياء، كلية العلوم، جامعة بغداد

[3]قسم الفيزياء، كلية التربية، الجامعة المستنصرية

الخلاصة

تم في هذه الدراسة استخدام حزمة ليزر النديميوم-ياك ذات التردد المضاعف و بتقنية المفتاح Q، ذات الطول الموجي 1064 نانومتر و ذات الطول الموجي 532 نانومتر و بمعدل تكرار 6 هيرتز، و زمن نبضة مقداره 10 نانو ثانية لترسيب الغشاء للمتراكب النانوي TiO_2 النقي و المخلوط مع العنصر النبيل Ag بنسب تراكيز مختلفة (10, 20, 30, 40 and 50) % wt. على قواعد من الزجاج و الوفر سليكون (111) باستخدام تقنية الترسيب بالليزر النبضي (PLD). عدة معلمات انماء اخذت بنظر الاعتبار لتحديد الشروط المثلى كتحديد درجة حرارة

القاعدة عند (300 ^{o}C)، ضغط الاوكسجين ($2.8x10^{-4}$)، طاقة الليزر (700 mJ)، عدد النبضات (400) نبضة و سمك الغشاء المرسب (170 nm). تم دراسة تضاريس السطح باستخدام مجهر القوة الذرية (AFM). و تظهر الدراسة بأن قيم RMS للاغشية الرقيقة و خشونة السطح ازدادت بزيادة محتوى الفضة، بينما الحجم البلوري قل بزيادة محتوى الفضة. تم قياس التحسسية لغاز NO_2 و NH_3 عند تراكيز مختلفة لكل جزء من المليون من الغاز (ppm). ان تحسسية اوكسيد التيتانيوم المخلوط مع العنصر النبيل الفضة اعلى مما في حالة اوكسيد التيتانيوم لوحده و المحضرة على قواعد من الزجاج و اعلى حساسية لغاز No_2 استطاع الغشاء تحسسها كانت بحدود 50% تقريبا للغشاء المتراكب النانوي $_{90\%}TiO_2/_{10\%}Ag$ عند افضل درجة حرارة تشغيل و كانت عند (200 ^{o}C). ان اضافة العنصر النبيل مثل الفضة جعل الاغشية المحضرة اكثر تحسسية لغاز NO_2.

Introduction

The market for resistive-type gas sensors is dominated by materials developed on the base of thin or thick layers composed of polycrystalline metal oxides. The nanostructures of different forms, i.e., nanowires, nanotubes, nanoflowers, have been shown to display better gas selectivity and sensitivity [1-3]. Additionally, open nanostructures facilitate the penetration of gas, and as a consequence, reduces the response time. Titanium dioxide (TiO_2) is effectively used in environmental and energy production applications such as dye-sensitized solar cells, photocatalytic water purification, and hydrogen generation by water splitting [4-6]. In sensor technology this n-type semiconductor is frequently considered as a promising material for gas detection applications [7]. In addition, Noble metals like Pt, Pd, Au, and Ag have been utilized to reduce the operation temperatures through effective improvements of the interaction between TiO_2 surface and the gas molecules [8-11]. Other studies addressed some limitations of the gas sensors by improving the structure and morphology of the gas sensor films. Sonker et al. [12] successfully prepared a nano-petal like NO_2 sensor through a cheap and easy chemical route. Plecenik et al. [13] constructed a highly-sensitive room-temperature semiconductor gas sensor based on nanoscale Pt-TiO_2-Pt sandwich.

In this study, we have prepared pure TiO_2 and its composite, which mixed with Ag, by PLD technique to produce high-quality TiO_2/Ag nanocomposite thin films. Special attention was paid to the influence of the processing parameters, such as mixing concentration on the morphology and Sensitivity properties of the films during the deposition.

Experimental

Titanium dioxide with a purity of 99.99% and silver with purity of 99.99% were mixed together at different concentration of x=0, 10, 20, 30, 40 and 50 wt. % using agate mortar then the mixture was pressed, using hydraulic manually type (SPECAC), under pressure of 6 tons for (5) minites to form a pellets of (2.8 cm) in diameter and (0.3 cm) thick. The pellets were sintered in air at temperature of (400 ºC) for 3 h. The TiO_2/Ag films were deposited on glass slides substrates of (1.5×1.5 cm^2). The substrate was cleaned with dilated water using ultrasonic process for 15 minute to deposit the films at 300 ºC. PLD technique was used to deposit the films under vacuum of (2.8×10^{-4} mbar) using Nd:YAG with (λ= 1064 nm) SHG Q-switching laser beam at 700 mJ, repetition frequency (6Hz) for 400 laser pulse is incident on the target surface making an angle of 45° with it. The distance between the target and the substrate was (2.5 cm). The substrate was heated under temperature (300 ºC).

Atomic Force Microscopy (AFM) is a widely used technique for investigating the surface

microstructure and quantifies surface topography. The grain size and surface roughness are investigated with a Nanoscope atomic force microscope in tapping mode. In this study, the morphological features of the various films are investigate with Angstrom Advanced AA3000 Scanning Probe Microscope (SPM), which manufacture in USA.

Gas sensor system

The process of determination the sensitivity parameter is mainly comprised in the response time and recovery time of the fabricated TiO_2/Ag gas sensor detector, for which a suitable setup is prepared for this purpose. Fig. 1. displays the system of gas sensor testing, which consists of a cylindrical stainless steel test chamber of diameter 30cm with a height of 35cm. The effective volume of the chamber is (6594) cc; it has an inlet for allowing the tested gas to flow in and an air admittance valve to allow the flow of atmospheric air after evacuation. At the base of the chamber, a multi-pin feed through allows the electrical connections to be established to the heater sensor electrodes, and K-type thermocouple.

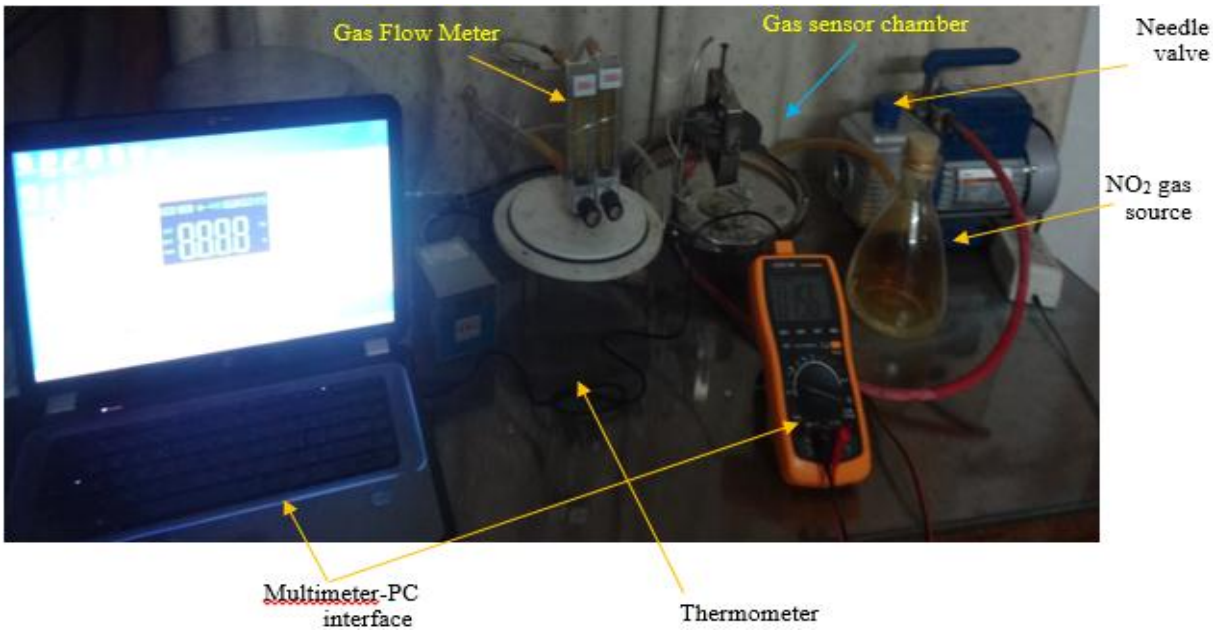

Fig.1: A photograph of gas sensor testing system.

The heater consists of a K-type thermocouple and a hot plate inside the chamber in order to make a control on their operating temperature of the sensor as shown in the Fig. 2. A UNI-T UT81B PC-interfaced digital multimeter, and Laptop PC, is used to register the variation of the sensor current when exposed to air-NO_2 gas mixing ratio. The gas mixing is fed through a tube over the sensor inside the test chamber to give the real sensitivity.

Sensitivity, *S*, is defined as the ratio of change of resistance in test gas $\Delta R = Ra - Rg$, to the value of resistance in air *Ra* where *Rg* is the sensor resistance in the presence of the test gas [14]:

$$S = \frac{\Delta R}{R_a} = \frac{R_a - R_g}{R_a} \quad (1)$$

where R_g is the electrical resistance of gas sensors and R_a is the electrical resistance of gas sensors in the air.

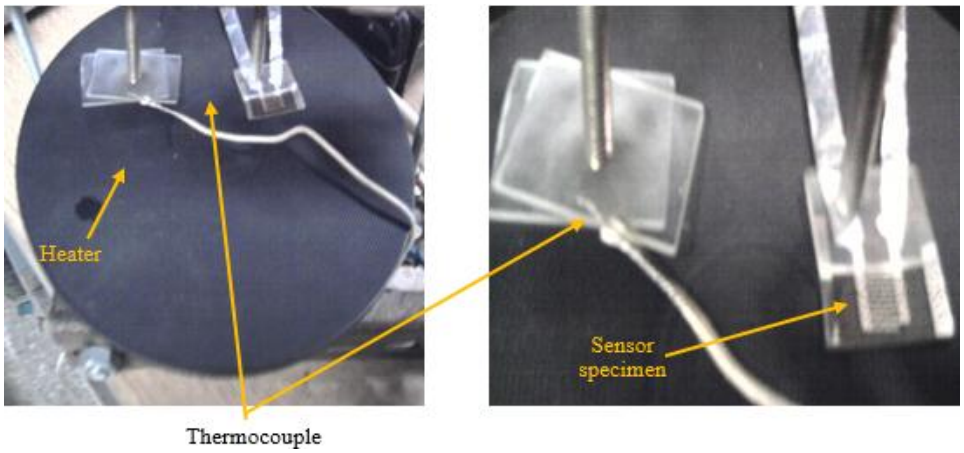

Fig. 2: Sample of gas sensor on heater plate.

Results and discussion

Fig. 3 shows the Atomic force microscopy images of TiO_2/Ag nanocomposite films deposited on glass substrate at (300 ºC) temperature. Figure show the surface topography (in two and three dimensional). As can be noticed from these, the films have high degree of homogeneity and consisted of small nanocrystalline grains, the surface morphology of TiO_2/Ag nanocomposite as observed from the Atomic force microscopy micrographs proves that the grains are uniformly distributed with individual grains extending as shown in Fig. 3. The surface roughness value and the root mean square, as in Table 1, observed surface roughness had random variation where it is increase at concentration ratio of Ag 10 % wt. while decrease at ratio (20 and 30)% wt. and then increase at ratio (40)% wt. and decrease at (50)%wt.. However, the roughness variation among these values may be considered random, and a specific contribution of Ag mixing to the roughness cannot be defined. The average grain size of nanocomposite pure TiO_2 thin film is calculated from AFM studies found to be equal to (55.26) nm and decreases with increasing of Ag concentration ratio.

Table 1: AFM characteristics of the TiO_2 films deposited at different Ag mixing ratio.

Samples	RMS (nm)	RS (nm)	Ten point height (nm)	Average G.S (nm)
TiO_2 - Pure	1.41	1.21	2.63	55.26
$_{90\%}TiO_2$:Ag $_{10\%}$	3.86	3.30	8.04	49.01
$_{80\%}TiO_2$: Ag $_{20\%}$	2.39	2.07	4.12	46.97
$_{70\%}TiO_2$: Ag $_{30\%}$	1.19	1.01	4.96	42.86
$_{60\%}TiO_2$: Ag $_{40\%}$	4.46	3.85	15.9	39.06
$_{50\%}TiO_2$: Ag $_{50\%}$	2.00	1.64	10.9	36.78

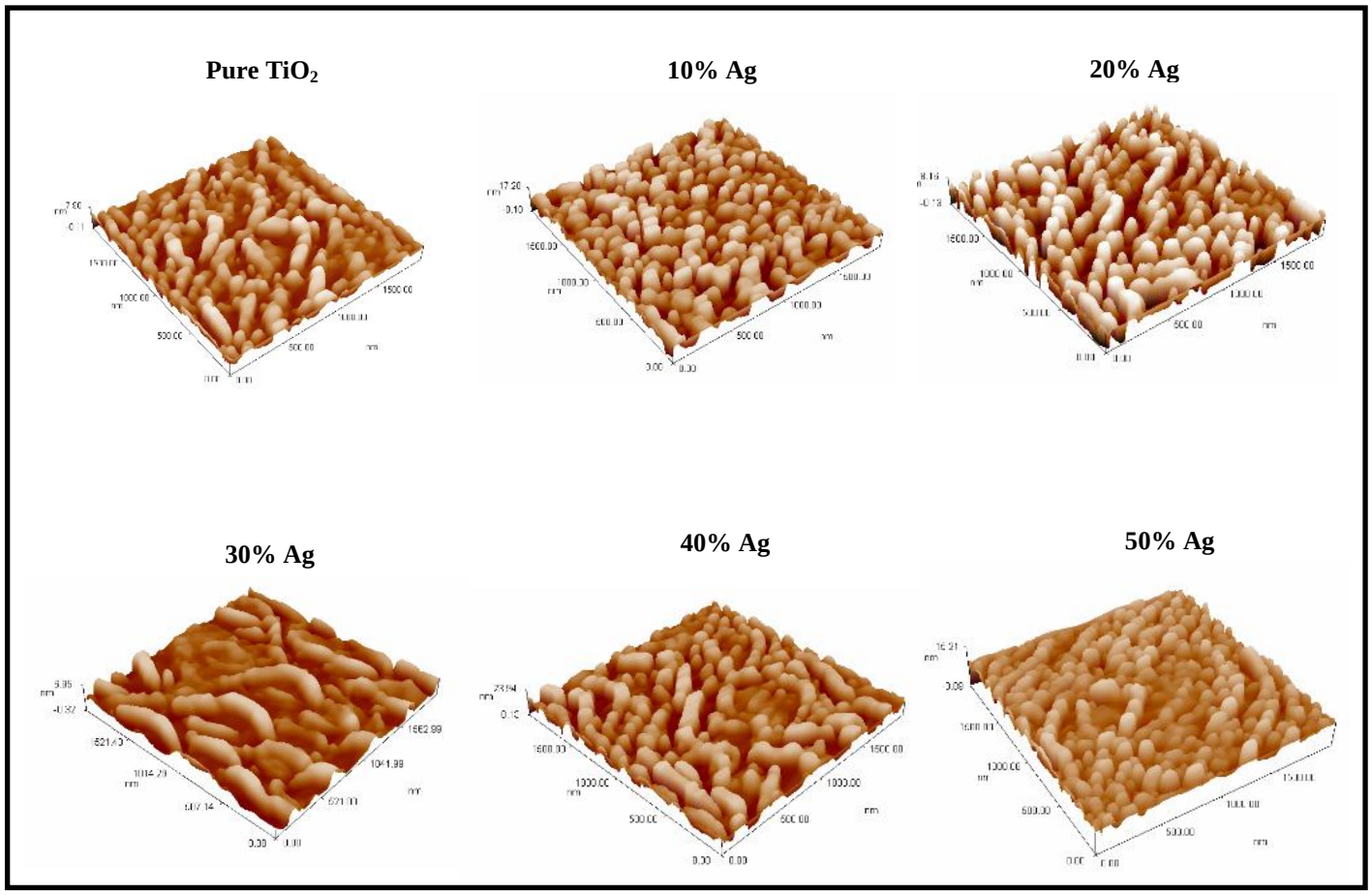

Fig. 3: AFM image of the TiO_2 films deposited at various Ag-concentration ratio at laser energy 700 mJ, O_2 pressure= 2.8×10^{-4} mbar.

Gas sensing measurement

Sensitivity with operation temperature

The film is initially tested to confirm its semiconducting behavior. The sensor is placed on a heater base and its resistance is measured as the temperature rises up from (25-300) ^{o}C in the dry air atmosphere. Figs. 4 and 5 show the variation of sensitivity as a function operation temperature in the range (25-300 ^{o}C) of the TiO_2 films with variance concentration ratios of Ag. The sensing test was done using 3% NO_2: air and 10%NH_3: air mixed ratio and bias voltage (6 V) were applied to the electrodes of all samples.

Fig. 4 is an illustration the sensitivity of TiO_2 composite sensor, as thin films, to 60 ppm of NO_2. The maximum sensitivity to NO_2 by pure TiO_2 sensor is about 7.55% at around (300) °C, [15, 16] but the $(TiO_2)_{90\%}(Ag)_{10\%}$ sensor displays a great enhancement of sensitivity to NO_2, especially at (200) °C where the sensitivity to 60 ppm of NO_2 reaches as high as (49.79%), more than 11 times more sensitive than that of pure TiO_2 sensor. It should also be noted that the optimum sensing temperature required for the maximum sensitivity is at around 200 °C for TiO_2 sensor [16] which is lower than that of pure TiO_2 sensor (~300 ^{o}C). Table 2 show the relation of sensitivity with temperature and concentration ratios of Ag in a pure TiO_2 and $(TiO_2)_{1-x}(Ag)_x$ nanocomposite thin films gas sensor with NO_2 test gas.

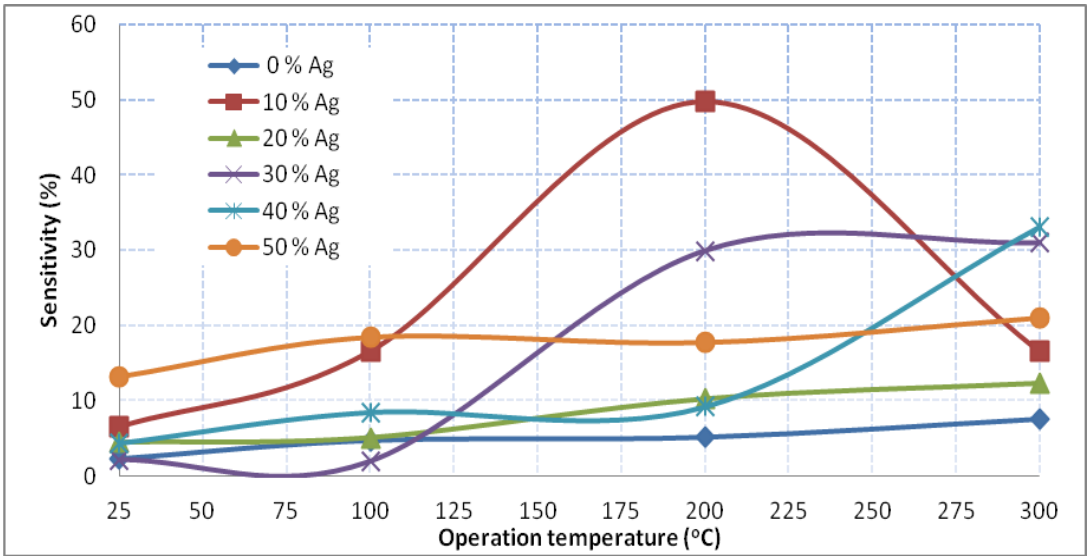

Fig. 4: The variation of sensitivity with the operating temperature for different Ag concentration in a pure TiO_2 and $(TiO_2)_{1-x}(Ag)_x$ nanocomposite thin films gas sensor with NO_2 test gas.

Table 2: The values of sensitivity of a pure TiO_2 and nanocomposite $(TiO_2)_{1-x}(Ag)_x$ thin films gas sensor with NO_2 test gas as a function of operation temperature and concentration ratios of Ag.

	Concentration ratios of Ag						
Temp. (°C)	**0%**	**10%**	**20%**	**30%**	**40%**	**50%**	
30	2.3162	6.5610	4.41915864	2.1848450	4.34899	13.261872	**Sensitivity (%)**
100	4.73037	16.5957	5.06306306	1.9581395	8.45161	18.472966	
200	5.1648	49.015	10.3162393	29.664363	9.1848	17.768759	
300	7.5558	16.5610	12.4191586	31.0137169	33.0679	21.02841918	

Fig. 5 shows NH_3 is used as the probing gas, similar results are obtained: the maximum sensitivity of $_{70\%}TiO_2/_{30\%}Ag$ composite sensor to 200 ppm of NH_3 can reach 20%, which is about 13 times higher than the sensitivity of pure TiO_2 sensor, and the optimum sensing temperature of TiO_2 composite sensor is at around (300) ^oC. Table 3 shows the relation of sensitivity with temperature and concentration ratios of Ag in a pure TiO_2 and $(TiO_2)_{1-x}(Ag)_x$ nanocomposite thin films gas sensor with NH_3 test gas.

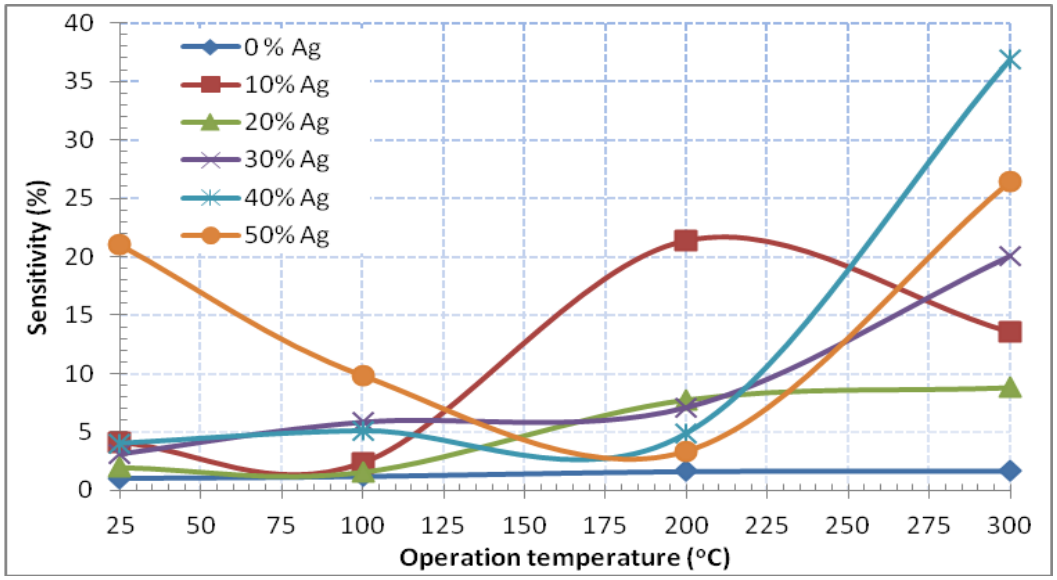

Fig. 5: The variation of sensitivity with the operating temperature for different Ag concentration in a pure TiO_2 and nanocomposite TiO_2/Ag thin films gas sensor with NH_3 test gas.

Table 3: The values of sensitivity of a pure TiO_2 and nanocomposite $(TiO_2)_{1-x}(Ag)_x$ thin films gas sensor with NH_3 test gas as a function of operation temperature and concentration ratios of Ag.

	Concentration ratios of Ag						
Temp. °C	**0%**	**10%**	**20%**	**30%**	**40%**	**50%**	
25	1.03573	4.07239	2.00364	3.13725	4.01837	21.0127	**Sensitivity (%)**
100	1.21089	2.32919	1.59798	5.85885	5.09554	9.84848	
200	1.63551	21.3612	7.75254	7.10696	4.86656	3.38189	
300	1.68855	13.5319	8.78926	20.0328	36.9365	26.4029	

All the above results have shown that the sensitivities of TiO_2 thin films as gas sensors to the oxidizing and reducing gases have been greatly enhanced.

AFM results have shown that, in the presence work, the $(TiO_2)_{1-x}(Ag)_x$ thin films has different cluster sizes. When the particle size of TiO_2 is small enough, especially the grain size is comparable to the depth of the sub-surface depletion layers, the whole resistance and sensitivity of the TiO_2 sensor are controlled by the grains themselves, inducing an inverse relationship between particle size and gas sensitivity [17, 18], with the smaller particle producing higher sensitivity.

Furthermore, it is well known that the conductivity of a semiconductor gas sensor is mainly determined by the presence of singly-charged oxygen vacancies [19] and the surface adsorbed oxygen species plays an important role during the sensing process [20].

The higher sensitivity may be attributed to the optimum surface roughness, porosity, large surface area and large rate of oxidation [21]. The maximum sensitivity of the TiO_2 with 10%Ag films to NO_2 gas is found to be 49% at 200 ^oC as showing in Fig. 4.

Fig. 5 show the variation of sensitivity with the operating temperature for different Ag concentration in a pure TiO_2 and nanocomposite TiO_2/Ag thin films gas sensor with NH_3 test gas.

Figs. 6 and 7 show the dependence of the sensor's sensitivity to the

content of Ag in TiO_2 thin films sensors. These figures show the sensitivities of pure TiO_2 sensor and different $(TiO_2)_{1-x}(Ag)_x$ sensors to 60 ppm of NO_2 in the temperature range (25 °C-300) °C. The maximum sensitivity of the pure TiO_2 sensor to 60 ppm of NO_2 is 4.55 % at (300) °C [22]. However, $(TiO_2)_{90\%}(Ag)_{10\%}$ sensor displays a great enhancement of sensitivity to NO_2: the maximum sensitivity can be achieved up to 49%, and the optimum temperature where the sensitivity is the maximum is at around (200) °C, which is lower than that of the pure TiO_2 sensor.

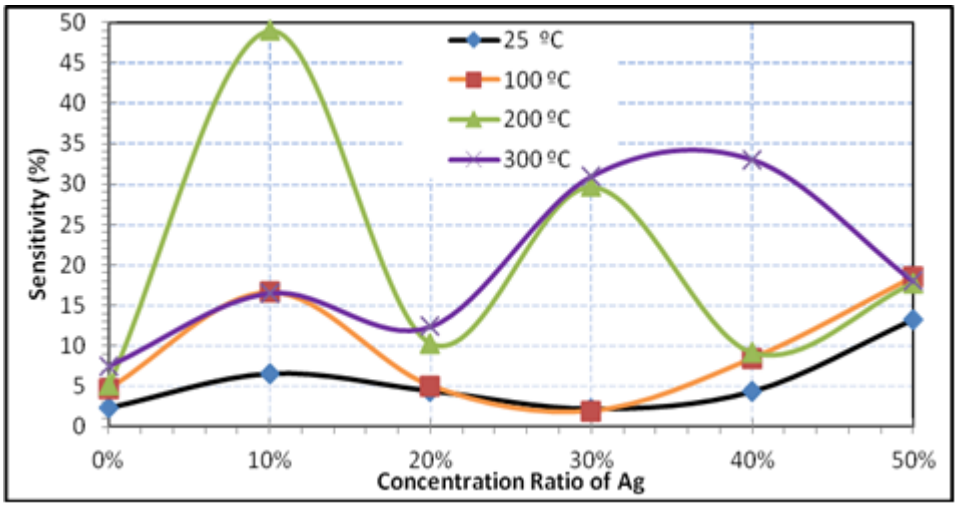

Fig. 6: The variation of sensitivity with different Ag concentration in a pure TiO_2 and $(TiO_2)_{1-x}(Ag)_x$ nanocomposite thin films gas sensor with NO_2 test gas.

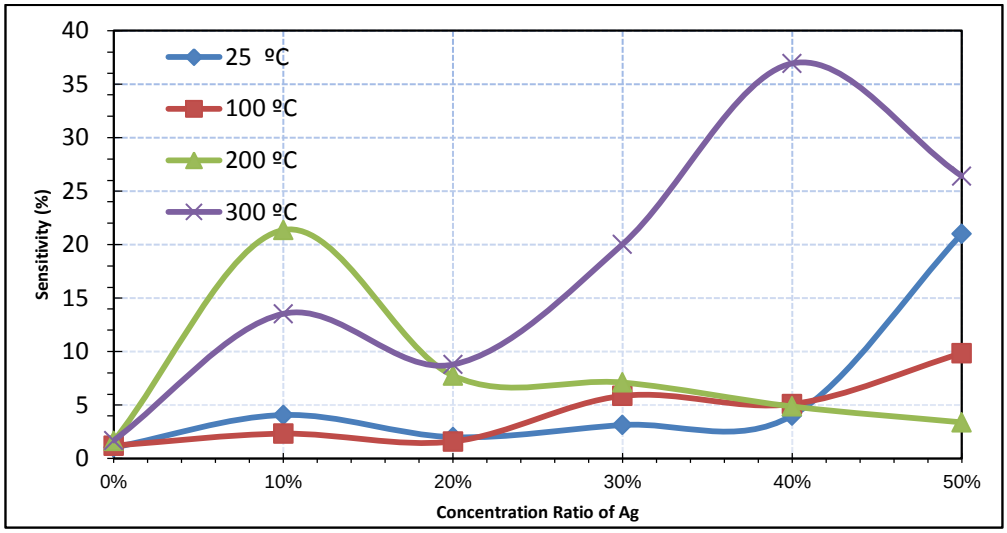

Fig. 7: The variation of sensitivity with different Ag concentration in a pure TiO_2 and $(TiO_2)_{1-x}(Ag)_x$ nanocomposite thin films gas sensor with NH_3 test gas.

Response time and recovery time

The response time and recovery time of the pure TiO_2 to wards 3% NO_2 and 10% NH_3 :Air gas mixing ratios has been explored. The successive tests are performed at a bias voltage of 6V and a 300 ^oC operating temperature. The results are shown in Figs. 8, and 9.

Fig. 8 indicates here both the response and recovery times of the TiO_2 gas sensor with (0, 10, 20, 30, 40 and 50) % Ag concentration ratios. The response and recovery time decreases with increasing Ag concentration to a minimum value at 40% Ag concentration and increased after that.

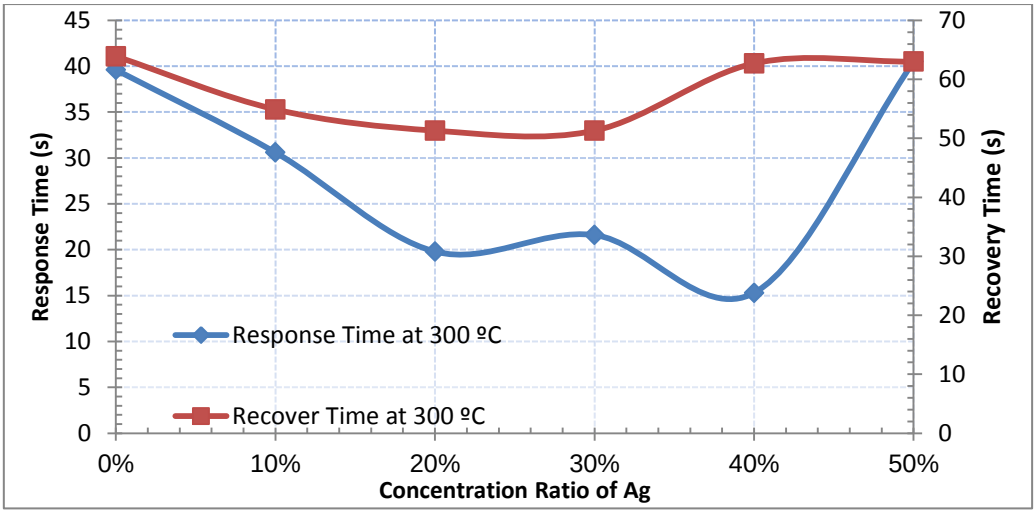

Fig. 8: The variation of response time and recovery time Ag concentration ratios in TiO_2 at optimum operating temperature (300 ºC) for NO_2 testing gas.

Fig. 9 shows the relation between the response and recovery time with Ag concentration ratio (deposition ratio of preparing sample) of optimum operating temperature of 10% NH_3:Air mixed ratio (test gas). The response and recovery time were decreased with increasing Ag content to 30% Ag and increase after that.

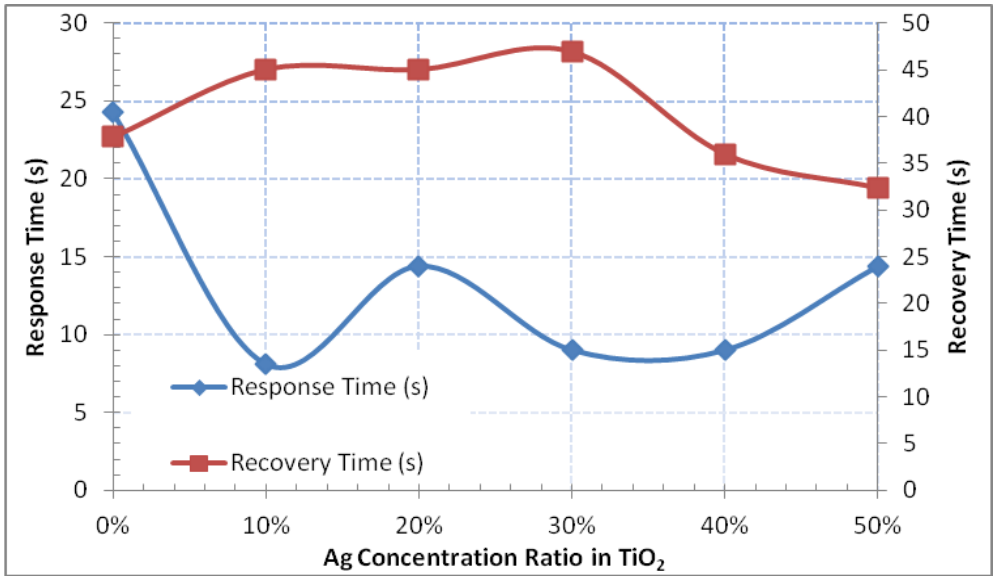

Fig. 9: The variation of response time and recovery time Ag concentration ratios in TiO_2 at optimum operating temperature (300 ºC) for NH_3 testing gas.

Gas sensing mechanism of TiO_2 pure and $(TiO_2)_{1-x}(Ag)_x$ thin films

Gas sensing mechanism depends on the surface reaction between chemisorbed oxygen, oxidant and reducing gases. The adsorption of oxygen on the film surface has two forms: physisorption and chemisorption. At elevated temperature, chemisorption is dominant. The transition from physisorption to chemisorption needs activation energy, which can be accomplished by increasing operating temperature. It has been reported that the amount of oxygen adsorbed on the sensor surface goes on increasing with an increase in temperature [23, 24].

Molecular oxygen and atomic oxygen have a dominant influence on the electrophysical and gas sensing characteristics of TiO_2 films in the temperature ranges of (25–300) ^oC, where the oxygen is adsorbed at the surface of the metal oxide that enables an electron trapping. Hence the charge carrier density is reduced which leads to an increase in the resistance of the TiO_2 Pure and $(TiO_2)_{1-x}(Ag)_x$ nanocomposite. This reaction can be expressed as follows [24]:

$$O_2\ (atm) + 2e^-\ (cond\ band) \rightarrow 2O^-\ (ads)$$

where O_2 is the adsorbed oxygen molecules, O^- is the chemisorbed oxygen and e^- are the trapped electrons from the TiO_2 Pure and $(TiO_2)_{1-x}(Ag)_x$ nanocomposite surface.

O^- Species on the surface, act as electron acceptors, and lead to the formation of depletion layer extending to the particles as well as surface barrier. This surface states and surface barrier play an important role for sensors, since it controls the electron transfer between particles, test gas and the sensing material, affecting the overall resistance. Exposure to NO_2 and NH_3 gases, with an elevated temperature, the reabsorbed oxygen species ($O^-\ surf$).

It results in the rising coverage of oxygen, binding more electrons to the conduction band of TiO_2, raising the barrier. This phenomenon increases the depletion region reducing the conductivity or enhancing the resistance [25].

Figs. 10 and 11 show the variation of resistance with time of TiO_2 Pure and nanocomposite TiO_2/Ag thin films as exposed to 3%(60l/h) NO_2 and 10%(200l/h) NH_3 in the air ambient injected into testing chamber and bias voltage is keeping at (6 V), at optimal operating temperature of each sample. The resistance is measured directly with time and the sensor resistance initially reaches the steady state before gas opening, in this time we open the gas to allow mixing with air inside the chamber. The resistance increases abruptly to reach a steady state then we switch the gas off. Then current returned to initial case. The ability of a sensor to sense the presence of gas depends on the nature of the interaction between the gas molecules and the surface atoms of the sensing film. The reactivity of the surface is critically dependent on its mixing and the defect structure.

Fig. 10 shows a rapid increase of the resistance with time for pure TiO_2 to reach a saturation state when the gas on, this may be due to a saturation of adsorption of a NO_2 gas on the surface. The resistance returns to the initial state when the gas off, the sensitivity of pure is (4.5%) calculate while the response and recovery time is (39.6 s), (63.9 s) are observed.

The maximum resistance that obtained (49 %) and achieved for (10% concentration ratio of Ag) with response and recovery time is (33.3 s), (51.3 s) respectively. We can conclude that the mixing of TiO_2 with Ag leads an unstable surface to the formation of bridging oxygen vacancies, the concentration of these bridging oxygen sites are the most energy favorable for NO_2 gas adsorption. The mixing Ag with TiO_2 structures is a possible way of gas adsorption by filling the bridging vacancy site with the gas atom. The binding energy (E.B) of the adsorbed gas atoms with the Ag mixed TiO_2 slab displays a maximum at a low concentration ratio of Ag and will cause strongly interaction with the surface and gas molecules that provide a robust change in sensor resistivity [26].

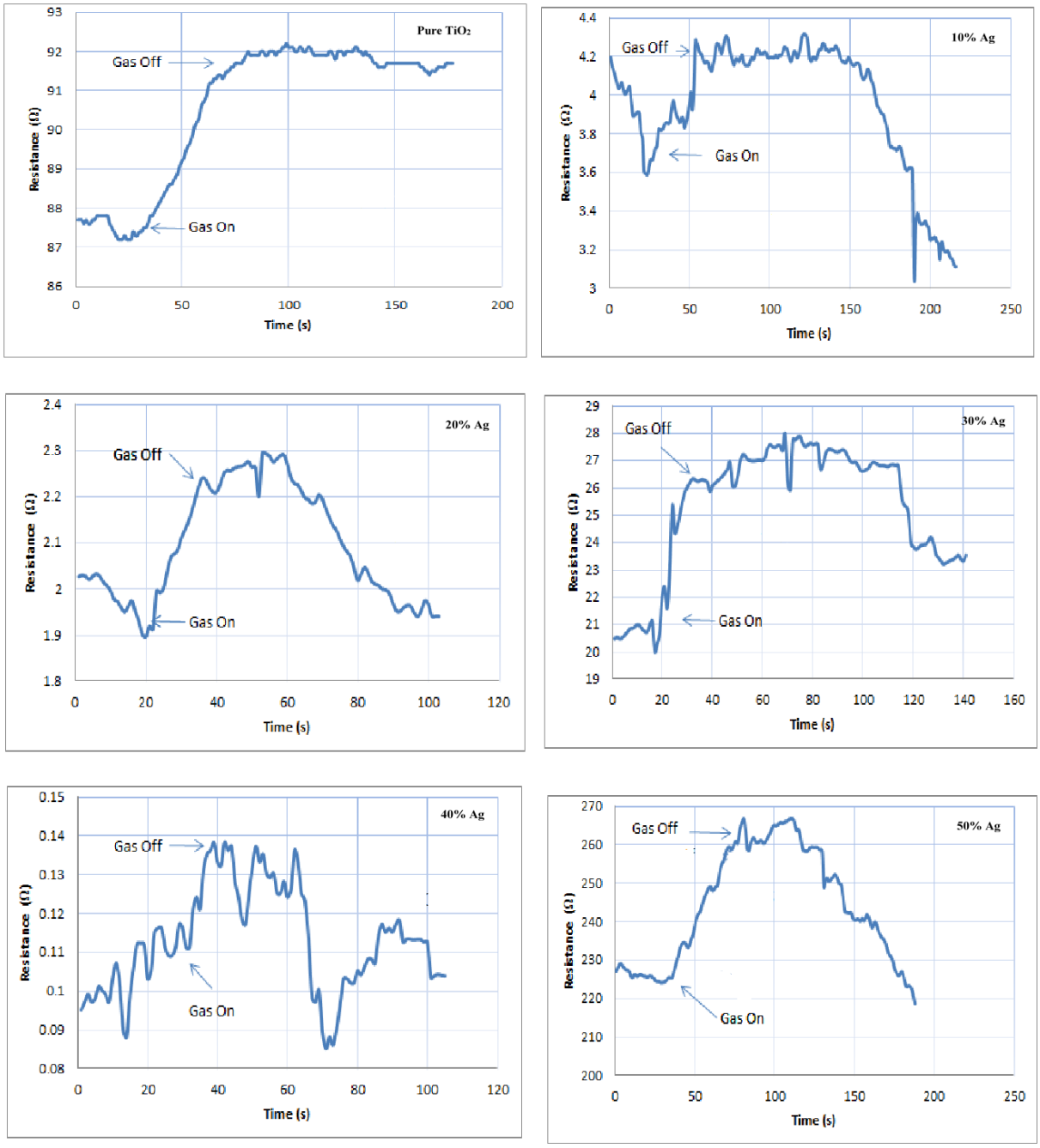

Fig. 10: The variation of resistance with a time of pure TiO_2 and (10, 20, 30, 40, and 50) concentration ratios of Ag as exposed to 3% mixing ratio NO_2: air and bias voltage of (6) V at optimum temperature (300) °C.

Fig. 11 shows that the low resistance (1.688%) for pure TiO_2 with fast response and recovery time (24.3 s), (37.8 s) respectively, while Fig. 7 exhibits the maximum resistance (36.9 %) and response and recovery time (9 s), (34.2 s) for 40% from mixing ratio of Ag with TiO_2. Decrease in sensitivity due to decrease in binding energy favorable between gas atoms with bridging oxygen sites.

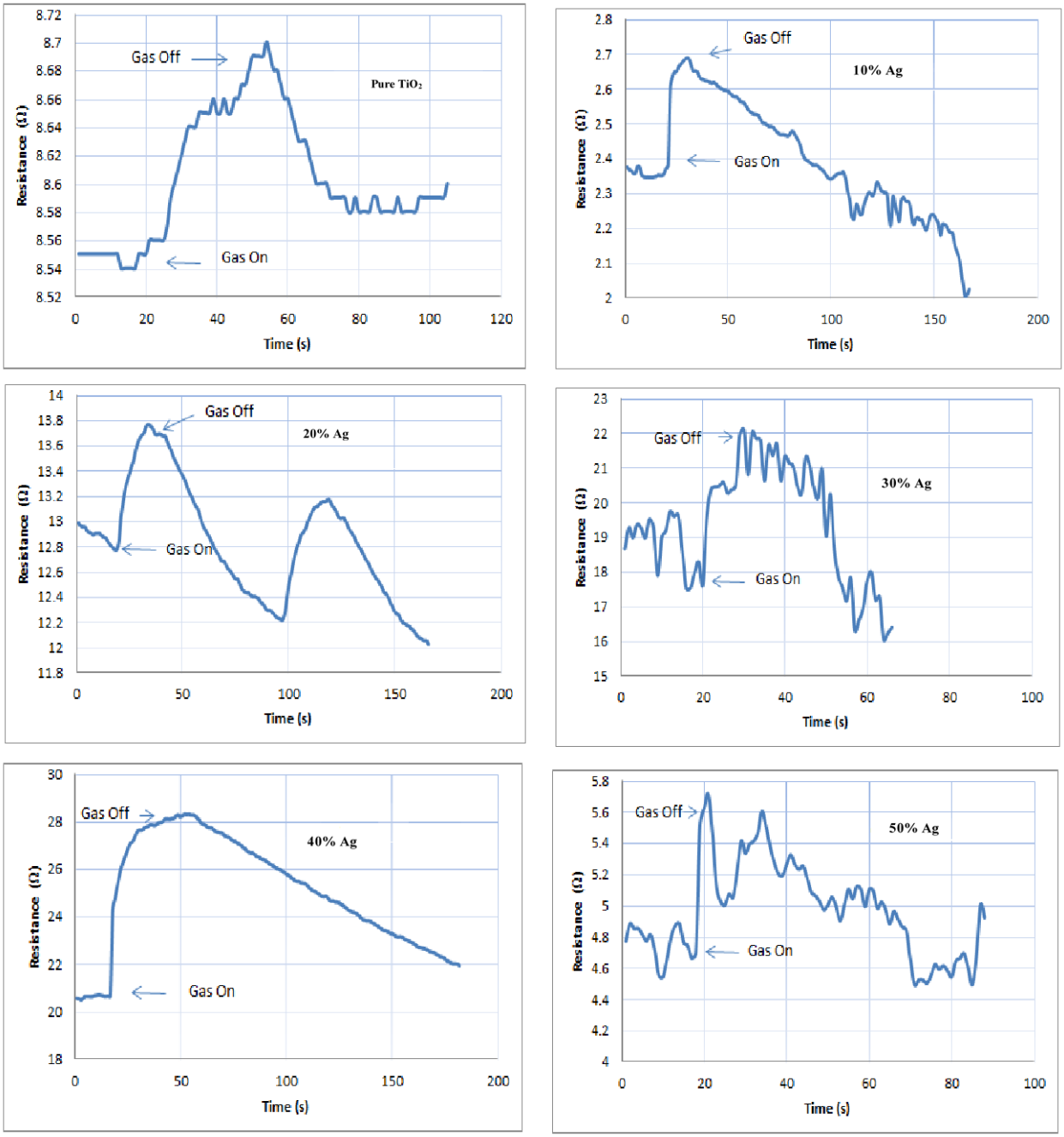

Fig. 11: The variation of resistance with a time of pure TiO_2 and variance concentration ratio of Ag as exposed to 10% mixing ratio NH_3: air at optimum temperature (300) °C.

The influence of gas concentration on sensitivity

The TiO_2 sensing samples are prepared at different conditions. Fig. 12 exhibit the transient response as a function of NO_2 gas concentration for the TiO_2 sensing element at (300) °C. The sensitivity of the TiO_2 gas sensor increases as the NO_2 gas concentration is increased from 20 to 60 liter/hour and it drops relatively rapidly when the NO_2 gas is removed , indicating that the gas sensor has a good response for different NO_2 concentrations. Besides, it takes almost the same time for the sensor to reach the maximum sensitivity for different NO_2 concentrations. This result is consistent with the conclusion for the dominance of operation temperature for the response time [22]. Both response and recovery time of the

sensor have the same behavior as the NO_2 target gas concentration increases. Both of them were decreased with increasing NO_2 concentration up to 60 l/h at which the lowest response and recovery times of (15 s) and (51 s) are observed. As it is apparent from the figure, the sensor sensitivity to NO_2 gas increased linearly with NO_2 test gas mixing ratio up to 60l/h. The maximum sensitivity record (36%) for the sample prepared.

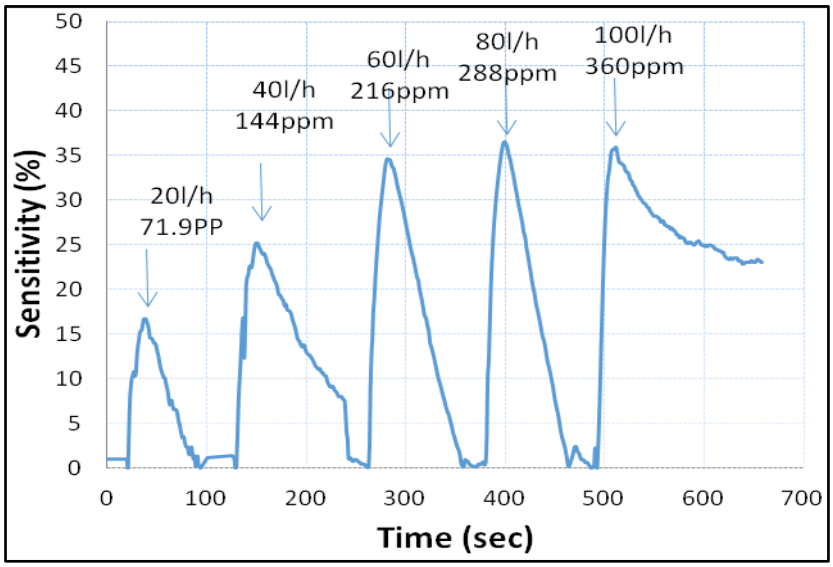

Fig. 12: The variation of sensitivity with time for different concentration with NO_2: air mixing ratio of nanocomposite TiO_2/ Ag thin films at a bias voltage of (6 V) and operating temperature (300) °C.

Figs. 13 and 14 represent the variation of sensitivity and a grain size with silver (Ag) mixing with titanium dioxide (TiO_2) of optimum operating temperature (300 ^oC). NH_3 reducing gas and NO_2 oxidant gas used as testing gases where mixing with air during test. Fig. 13 shows as NO_2 used as testing gas, the grain size was decreased with Ag mixing concentration from 0% concentration to 20%, from 20% Ag to 40% the grain size not high stall with small variation, after that from 40% Ag to 50% grain size increased. The sensitivity increased as grain size decreased, where the maximum sensitivity shows with grain size (42.86, 39.06 nm) at (30%, 40% concentration ratio of Ag) as shown in Fig.13.

Fig.14 shows as NH_3 used as testing gas, the sensitivity was increased with concentration ratio of Ag increased in (0-10)% and from (20-40)% while the sensitivity was decreased at concentration ratio of Ag in tow regain, first regain beyond 10% to 20% and second regain between (40-50) % wt. This figure, also, show that the grain size decreased with increased Ag mixing where, the sensitivity increased as grain size decreased, where the maximum sensitivity shows with grain size (39.06 nm) at (40% mixing) as shown in Fig. 14.

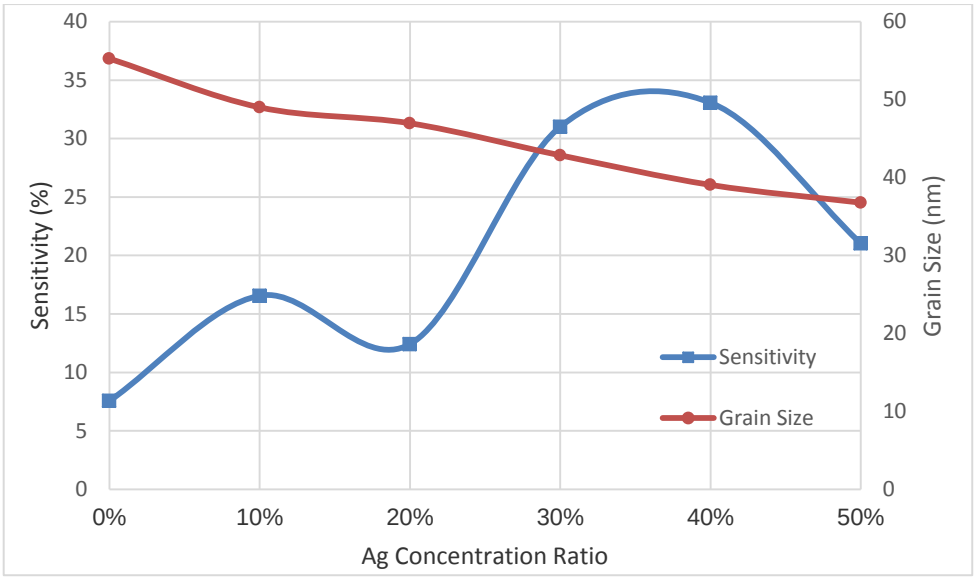

Fig. 13: The variation of grain size and sensitivity with Ag concentration ratio at optimum operating temperature (300 °C) for NO_2 testing gas.

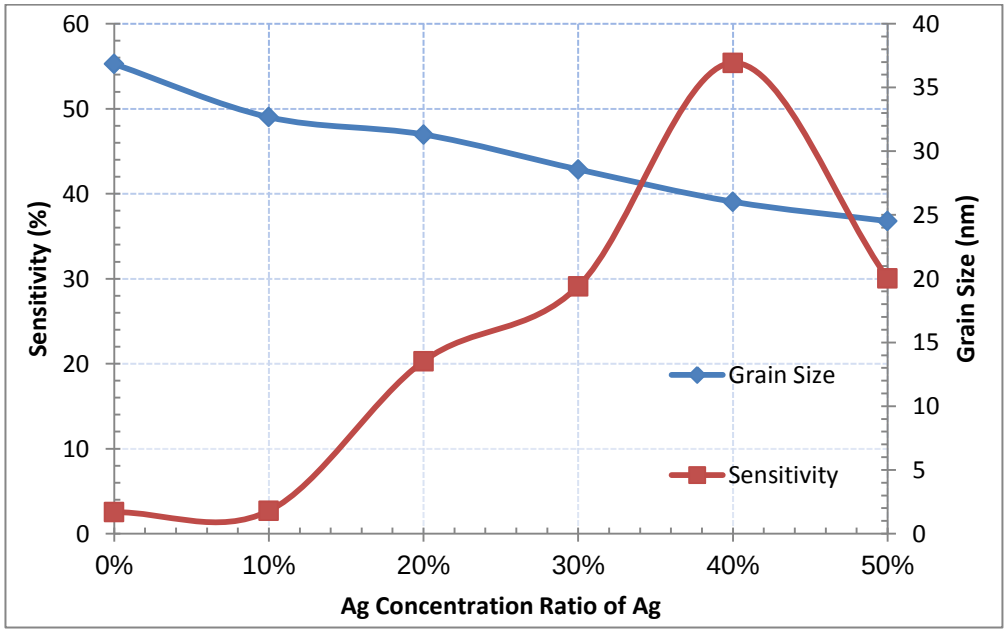

Fig. 14: The variation of grain size and sensitivity with Ag concentration ratio at optimum operating temperature (300 °C) for NH_3 testing gas.

The reduction in the grain size allows the space charge to cover large volume of the grain and the large number of grain boundaries providing large area for adsorption oxygen. Hence large variation in the barrier and resistance can enhance the reactivity at optimum mixing ratio. Also, the density of surface states increases with reduction in the particle size hence, the density of surface states can help in higher sensitivity. The relationship of sensitivity of NO_2 and NH_3 with Concentration ratio of Ag and grain size were showed in Table 4.

Table 4: The effect of Ag concentration ratio into both sensitivity and grain size.

Concentration ratio of Ag (%)	Sensitivity for NO_2 (%)	Sensitivity for NH_3 (%)	G.S (nm)
10	4.555809	1.688555	55.26
20	16.56104	13.53191	46.97
30	12.41916	1.789264	39.06
40	32.01372	20.03284	42.86
50	33.06796	37.9365	36.78

Conclusions

Nanocomposites TiO_2/Ag films prepared by using pulsed laser deposition techniques on the glass and and p-Si wafer (111) substrate exhibits a uniform growth of nanocrystalline films. The surface topography characteristics of all films studied by the Atomic Force Microscope (AFM) show that there is a decreasing in average grain size while the average surface roughness increased with increasing of the Ag contents in TiO_2. Nanocomposites TiO_2/Ag films sensors demonstrated high sensitivity and relatively fast to NO_2 Oxidized gas. Thus, they exhibit decrease in the conductance for exposure to NO_2 gas of different concentrations for (ppm) and operating temperatures, showing excellent sensitivity. It is found that the sensing of NO_2 and NH_3 gas in noble metal Ag sensors is related to the enhancement of adsorption of atmospheric oxygen. The variation of the operating temperature of the films leads to a significant change in the sensitivity of the sensor with an ideal operating temperature of about 200 ºC was 49.79% a for NO_2 gas with 10%Ag films, while highest response obtained for NH_3 gas (36.93%) was at a concentration ratio 40% Ag at an operation temperature of 300 ºC after which sensor sensitivity decreases. The fast response and recovery time at this point are coming from at 40% Ag concentration at time 15s and 23.4s with NO_2 gas, while fast response time (7s) and recovery time of (12s) with NH_3 gas at 40% Ag concentration comparing to other samples.

References

[1] P. Rai, S. Raj, K. J. Ko, K. K. Park, Y. T. Yu, Sensors Actuators, B Chem., 178, 2 (2013) 107-112.

[2] W. Maziarz, T. Pisarkiewicz, A. Rydosz, K. Wysocka, G. Czyrnek, Proc. of Spie., 8902 (2013) 1-8.

[3] K. Nakata and A. Fujishima, J. Photochem. Photobiol. CPhotochem. Rev., 13, 3 (2012) 169-189.

[4]Q. Zhang, E. Uchaker, S. L. Candelaria, G. Cao, Chem. Soc. Rev., 42 (2013) 3127-3171.

[5] Q. Zhang and G. Cao, Nano Today, 6, 1 (2011) 91-109.

[6] G. Eranna, Metal oxide nanostructures as gas sensing devices; CRC Press: Boca Raton, FL, U.S.A., 2012.

[7] Wojciech Maziarz, Anna Kusior, Anita Trenczek-Zajac, Beilstein J. Nanotechnol., 7 (2016) 1718-1726.

[8] T. Plecenik, M. Moško, A.A. Haidry, P. Durina, M. Truchlý, B. Granˇciˇc, M. Gregor, T. Roch, L. Satrapinskyy, A. Mošková, M. Mikula, P. Kús, A. Plecenik, Sens. Actuators B Chem., 207 (2015) 351-361.

[9]H. Kobayashi, K. Kishimoto, Y. Nakato, H. Tsubomura, Sens. Actuators B Chem., 13 (1993) 125-127.

[10] R.M. Walton, H. Liu, J. L. Gland, J.W. Schwank, Sens. Actuators B Chem., 41 (1997) 143-151.

[11] G.K. Mor, O.K. Varghese, M. Paulose, K.G. Ong, C.A. Grimes, Thin Solids Films, 496 (2006) 42-48.

[12] R.K. Sonker, S.R. Sabhajeet, S.Singh, B.C. Yadav, Mater. Lett., 152 (2015) 189-191.
[13] Xiaoying Peng, Zhongming Wang, Pan Huang, Xun Chen, Xianzhi Fu, Wenxin Dai, Sensors, 16, 1249 (2016) 1-14.
[14] R. C. V Gopal, S. V Manorama, V. J. Rao, C. V. G. Reddy, J. Mater. Sci. Lett., 9, c (2000) 775-778.
[15] Z. Wen and L. Tian-mo, Phys. B Condens. Matter, 405, 5 (2010) 1345-1348.
[16] K. I. Shimizu, K. Kashiwagi, H. Nishiyama, S. Kakimoto, S. Sugaya, H. Yokoi, A. Satsuma, Sensors Actuators, B Chem., 130, 2 (2008) 707-712.
[17] S. G. Ansari, P. Boroojerdian, S. R. Sainkar, R. N. Karekar, R. C. Aiyer, S. K. Kulkarni, Thin Solid Films, 295, 1–2 (1997) 271-276.
[18] F. Ren, L. Huang, Y. Ling, J. Feng, Sensors Actuators, B Chem., 148, 1 (2010) 195-199.
[19] K. Iijima, M. Goto, S. Enomoto, H. Kunugita, K. Ema, M. Tsukamoto, N. Ichikawa, H. Sakama, J. Lumin., 128, 5–6 (2008) 911-913.
[20] M. Setvín, U. Aschauer, P. Scheiber, Y.-F. Li, W. Hou, M. Schmid, A. Selloni, U. Diebold, Science, 341, 6149 (2013) 988-991.
[21] N. Bahadur, K. Jain, R. Pasricha, S. Chand, Sensors Actuators B. Chem., 159, 1 (2011) 112-120.
[22] L. Sivachandiran, F. Thevenet, P. Gravejat, A. Rousseau, Appl. Catal. B Environ., 142–143, 2 (2013) 196-204.
[23] P. Shankar, J. Bosco, B. Rayappan, Sci. Jet, 4, 126 (2015) 1-18.
[24] R. R. Salunkhe, V. R. Shinde, C. D. Lokhande, Sensors Actuators, B Chem., 133, 1 (2008) 296-301.
[25] Z. A. Ansari, T. G. Ko, J. Oh, IEEE Sens. J., 5, 5 (2005) 817-824.
[26] T. M. Inerbaev, Y. Kawazoe, S. Seal, J. Appl. Phys., 107, 10 (2010) 104504-104507.